

**COMPARISON OF INTERNAL DOSIMETRY
EVALUATION OF FLUORINE-18
FLUORODEOXYGLUCOSE (^{18}F -FDG) FOR
POSITRON EMISSION TOMOGRAPHY (PET)
USING OLINDA/EXM AND GEANT4 MONTE
CARLO SIMULATION**

MUHAMMAD ZULFADHLI BIN ZAINI

UNIVERSITI SAINS MALAYSIA

2025

**COMPARISON OF INTERNAL DOSIMETRY
EVALUATION OF FLUORINE-18
FLUORODEOXYGLUCOSE (¹⁸F-FDG) FOR
POSITRON EMISSION TOMOGRAPHY (PET)
USING OLINDA/EXM AND GEANT4 MONTE
CARLO SIMULATION**

by

MUHAMMAD ZULFADHLI BIN ZAINI

**Thesis submitted in fulfilment of the requirements
for the degree of
Master of Science**

March 2025

ACKNOWLEDGEMENT

All praises to Allah, peace and blessings be upon the Messenger of Allah S.A.W. for giving me strength to successfully complete this study. Millions of appreciations to my main supervisor Dr. Nurul Hashikin Ab. Aziz for her guidance, support, knowledge, and experience shared with me throughout this study. A big thanks to Ministry of Health for providing me a scholarship for my Master of Science in Medical Physics.

I would like to thank all the staff in nuclear medicine department, National Cancer Institute, who were involved directly and indirectly, especially physicists and technologists, in this study. A special thanks to senior physicist, Mr. Mohamad Aminudin who love to share his experience in dosimetry work with me.

My family members hold the utmost priority in my life, and I express my heartfelt gratitude to them for their unwavering support throughout this journey.

Thank You

TABLE OF CONTENTS

ACKNOWLEDGEMENT	ii
TABLE OF CONTENTS	iii
LIST OF TABLES	vi
LIST OF FIGURES	vii
LIST OF SYMBOLS AND UNITS	ix
LIST OF ABBREVIATIONS	x
ABSTRAK	xii
ABSTRACT	xiv
CHAPTER 1 INTRODUCTION	1
1.1 Background of the Study	1
1.2 Problem Statement	3
1.3 Aim & Objectives.....	4
1.4 Scope of study	4
1.5 Limitation of study	5
1.6 Thesis organization	5
CHAPTER 2 LITERATURE REVIEW	6
2.1 Cancer in Malaysia.....	6
2.1.1 Epidemiology of Cancer in Malaysia.....	7
2.1.2 Diagnosis of Cancer	7
2.1.3 Treatment Options for Cancer	8
2.2 Radioactive Decay.....	9
2.2.1 Alpha (α) decay	9
2.2.2 Beta (β) decay	9
2.2.3 Gamma (γ) decay	10
2.2.4 Positron emission (β^+) decay.....	11

2.3	Linear energy transfer (LET)	11
2.4	Radionuclide Production	12
2.5	Introduction to Nuclear Medicine	14
2.5.1	Type of Radiopharmaceuticals.....	15
2.5.2	Nuclear Medicine Modalities	17
2.6	Medical Internal Radiation Dosimetry (MIRD).....	18
2.6.1	Absorbed Dose, D	19
2.6.2	Activity.....	21
2.6.3	Cumulative Activity	22
2.6.4	Residence Time and Effective Half-Life	23
2.6.5	Organ absorbed dose by OLINDA/EXM.....	25
2.7	ICRP Dose limit for patients from radiopharmaceuticals	26
2.8	Monte Carlo Simulation	28
2.8.1	Generation of Mathematical Phantom in Monte Carlo simulations	30
CHAPTER 3 METHODOLOGY.....		32
3.1	Flow of study.....	32
3.2	Phase 1: Data collection	34
3.2.1	Patient criteria	34
3.2.2	Patient demographic	34
3.2.3	Data extraction	35
3.3	Phase 2: Imaging data analysis.....	35
3.4	Patient dosimetry analysis.....	38
3.4.1	Dosimetry by OLINDA/EXM.....	38
3.4.1(a)	Determination of Organ Uptake Fraction	39
3.4.1(b)	Determination of Residence time	40
3.4.1(c)	Determination of Absorbed dose	43
3.4.2	Dosimetry by Monte Carlo simulation.....	44

3.4.2(a)	Determination of Internal Organ Dose – Geant4 Monte Carlo Simulation	45
3.4.2(b)	Mathematical phantom Geometry	45
3.4.2(c)	Determination of number of events (N) per simulation	46
3.4.2(d)	Determination of characteristics of simulation.....	47
3.4.2(e)	Determination of absorbed dose in Geant4	48
CHAPTER 4	RESULT AND DISCUSSION.....	51
4.1	Dosimetry by calculation	51
4.1.1	Internal organ dose	51
4.1.1(a)	Uptake fraction	51
4.1.1(b)	Residence time.....	57
4.1.1(c)	Internal organ – Absorbed dose.....	60
4.1.2	Internal organ dose – MC Simulation – Geant4.....	63
4.1.2(a)	Specific absorbed dose	64
4.2	Comparison between absorb dose OLINDA/EXM 1.0 with MC simulation	65
CHAPTER 5	CONCLUSION AND FUTURE RECOMMENDATIONS.....	74
5.1	Conclusion.....	74
	Recommendations for future study	75
REFERENCES.....		76

LIST OF TABLES

	Page
Table 2.1	Common types of radionuclides sources..... 13
Table 3.1	Extraction data from the PET/CT imaging and dosimetry analysis...35
Table 4.1	Mean activity uptake fraction of ^{18}F -FDG per organ (activity at time per administered activity).53
Table 4.2	Residence time result of this study.....57
Table 4.3	Comparison of the organ residence time (h).58
Table 4.4	Result of organ absorbed dose in this study for 30 patients.....61
Table 4.5	Comparison of absorbed dose (mGy/MBq) among related studies. ...62
Table 4.6	Result of organ absorbed dose in 30 patients.....64
Table 4.7	Organ dose from OLINDA/EXM and Monte carlo simulations.....66

LIST OF FIGURES

	Page
Figure 2.1	The impact of the radionuclide half-life on cumulative patient dose is illustrated in this diagram. Since radioactive decay is exponential, the area under the curve (AUC) is simply $AUC = Dose/\lambda$ where λ is $\ln 2$ divided by the half-life..... 13
Figure 2.2	Time activity graph.22
Figure 2.3	Graph of area under the curve is equal to area of rectangle.....23
Figure 3.1	Flow chart of the study.....33
Figure 3.2	Example of patient images in Coronal (X), sagittal (Y) and transverse (Z) on CT, PET and fused PETCT showing the drawing of VOI on 3 organs.....36
Figure 3.3	Example of VOI statistic result from MIM software.....37
Figure 3.4	Diagram of dosimetry by using OLINDA/EXM.39
Figure 3.5	The main interface of OLINDA/EXM software.40
Figure 3.6	Nuclide input form tab.41
Figure 3.7	Model input form tab.41
Figure 3.8	Kinetic input form tab.42
Figure 3.9	Fit data to model feature.43
Figure 3.10	Absorbed dose result.44
Figure 3.11	Diagram of dosimetry using Geant4 MC simulation.45
Figure 3.12	Image of interface MIRD5 phantom in Geant4 software. (A) display MIRD5 Phantom. (B) shows the output of changing code of the phantom. (C) list of command in the phantom.46
Figure 3.13	The arrow shows the line code where the number of disintegrations, N need to be placed to run simulation in Geant4.47
Figure 3.14	Kinetic input of 2 organs.....48

Figure 3.15	Shows the processing of code in MIRD5 Phantom in Geant4 software.	49
Figure 3.16	Shows the result after processing of code in MIRD5 Phantom in Geant4. The units of absorb dose in organ are in MeV.	49
Figure 4.1	Uptake fraction versus time for organ liver male.....	53
Figure 4.2	Uptake fraction versus time for organ liver female.	54
Figure 4.3	Uptake fraction versus time for organ kidneys male.	54
Figure 4.4	Uptake fraction versus time for organ kidneys female.	55
Figure 4.5	Uptake fraction versus time for organ urinary bladder male.	56
Figure 4.6	Uptake fraction versus time for organ urinary bladder female.	56
Figure 4.7	Comparison of organ residence time.....	59
Figure 4.8	R2 statistical results for organ kidney	69
Figure 4.9	R2 statistical results for organ urinary bladder	69
Figure 4.10	R2 statistical results for organ liver	70
Figure 4.11	Bland Altman plot for organ urinary bladder.....	71
Figure 4.12	Bland Altman plot for organ kidneys.....	72
Figure 4.13	Bland Altman plot for organ Liver.....	72

LIST OF SYMBOLS AND UNITS

α	Alpha
β	Beta
γ	Gamma
β^+	Positron
L_{∞}	Linear energy transfer
Gy	Gray
^{99m}Tc	Technetium – 99m
^{18}F	Flourine - 18
Tc99m – DTPA	Technetium 99m – Diethylene – Triamine – Pentaacetate
Q(L)	Quality factor

LIST OF ABBREVIATIONS

WHO	World Health Organization
MNCRR	Malaysia National Cancer Registry Report
IKN	Institut Kanser Negara
NM	nuclear medicine
SPECT	Single-photon emission computed tomography
SPECT/CT	Single-photon emission computed tomography/computed tomography
PET	Positron emission tomography
PET/CT	Positron emission tomography/computed tomography
PET/MRI	Positron emission tomography/magnetic resonance imaging
MC	Monte carlo
RADAR	Radiation Dose Assessment Resources
MIM	Medical Image Merge
OLINDA/EXM	Organ Internal Dose Assessment/ Exponential Modelling
LET	Linear energy transfer
IXRPC	International X-ray and Radium Protection Committee
ICRU	International Commission on Radiation Units and Measurements
MIRDOSE	Medical International Radiation Dose
SAGE	Scientific Advisory Group for Emergencies
GEANT4	Geometry and Tracking 4
MCNP	Monte Carlo N-Particle
FLUKA	Fluktuierende Kaskade
EGSnrc	Electron gamma shower (National Research Council of Canada)
GATE	Geant4 Application for Tomographic Emission
GE	General Electric
CTAC	CT attenuation correction
2D	2-dimension

3D	3-dimension
TOF	time-of-flight
FWHM	full width at half maximum
ROI	region of interest
VOI	volume of interest
^{18}F – FDG	Flourine – 18 – Fluorodeoxyglucose
WBS	Whole body scan
MySCan	Malaysia Study on Cancer Survival
AAPM	The American Association of Physicists in Medicine
ORNL	Oak Ridge National Laboratory

**PERBANDINGAN PENILAIAN DOSIMETRI DALAMAN FLUORIN-18
FLUORODEOKSIGLUKOSA (¹⁸F-FDG) UNTUK PENGIMEJAN
TOMOGRAFI PANCARAN POSITRON (PET) MENGGUNAKAN
OLINDA/EXM DAN SIMULASI MONTE CARLO GEANT4**

ABSTRAK

PET/CT dengan ¹⁸F-FDG semakin banyak digunakan untuk pengimejan diagnostik, menjadikan penilaian dosimetri penting untuk mengurangkan pendedahan radiasi yang tidak perlu kepada organ lain. Kajian ini bertujuan untuk membandingkan dan menilai dos yang diserap kepada pesakit yang menjalani pengimejan PET/CT berurutan ¹⁸F-FDG dalam IKN menggunakan OLINDA/EXM dan simulasi Geant4 MC, memfokuskan pada mengenal pasti kaedah yang paling sesuai untuk aplikasi klinikal dan menganalisis sama ada dos yang diserap mematuhi dengan standard keselamatan yang ditetapkan oleh ICRP 128. Kajian ini melibatkan analisis retrospektif ke atas 30 pesakit dewasa termasuk 13 lelaki dan 17 wanita dengan purata umur, berat dan aktiviti yang ditadbir adalah 55.10 ± 14.05 tahun, 68.87 ± 20.99 kg dan 327.61 ± 87.95 MBq masing-masing. Perisian OLINDA/EXM versi 1.1 dan simulasi MC Geant4 (versi 10.6.0) digunakan untuk menilai dos yang diserap ke hati, buah pinggang dan pundi kencing. Fantom matematik MIRD5 digunakan dalam simulasi Geant4 MC manakala dalam OLINDA/EXM, model lelaki dan wanita dewasa yang jisim organ telah dinormalisasi dengan model rujukan Jepun telah digunakan. Purata dos yang diserap ke hati, buah pinggang dan pundi kencing ialah 0.010 ± 0.006 mGy/MBq, 0.011 ± 0.004 mGy/MBq dan 0.025 ± 0.047 mGy/MBq, masing-masing untuk OLINDA/EXM. Untuk simulasi Geant4 MC, purata dos yang diserap ke hati, buah pinggang dan pundi kencing ialah 0.009 ± 0.004 mGy/MBq,

0.011 ± 0.003 mGy/MBq dan 0.073 ± 0.086 mGy/MBq, masing-masing. Perbezaan yang sepadan antara kedua-dua kaedah ini ialah 10.53%, 0% dan 97.96% masing-masing untuk hati, buah pinggang dan pundi kencing. Kolerasi yang baik diperhatikan antara dos yang diserap dalam hati dan buah pinggang; walau bagaimanapun, Geant4 melebihi dos yang diserap dalam pundi kencing. Percanggahan ini disebabkan oleh perbezaan dalam kaedah yang digunakan untuk mengira dos yang diserap, isipadu pundi kencing yang tidak homogen, dan variasi dalam separuh hayat berkesan organ. Kedua-dua OLINDA/EXM dan Geant4 menunjukkan anggaran dos yang diserap yang boleh dipercayai, kerana hasilnya adalah dalam persetujuan yang baik antara kedua-dua kaedah. Walaupun OLINDA/EXM menawarkan antara muka yang lebih mesra pengguna, ia terhad dari segi fleksibiliti untuk mensimulasikan dos yang diserap dalam pelbagai persediaan klinikal lain. Geant4 sebaliknya, membenarkan fleksibiliti dalam mensimulasikan pelbagai persediaan dosimetri, namun terhad dari segi antara muka mesra pengguna, terutamanya dalam tetapan klinikal. Kesimpulannya, dos yang diserap yang direkodkan dalam kajian ini mematuhi had yang disediakan oleh ICRP-128, iaitu, 0.021 mGy/MBq, 0.017 mGy/MBq, dan 0.130 mGy/MBq, masing-masing untuk hati, buah pinggang dan pundi kencing, menunjukkan penggunaan selamat ¹⁸F-FDG untuk tujuan diagnostik di IKN.

**COMPARISON OF INTERNAL DOSIMETRY EVALUATION OF
FLUORINE-18 FLUORODEOXYGLUCOSE (18F-FDG) FOR POSITRON
EMISSION TOMOGRAPHY (PET) USING OLINDA/EXM AND GEANT5
MONTE CARLO SIMULATION**

ABSTRACT

PET/CT with ^{18}F -FDG is increasingly used for diagnostic imaging, making dosimetry evaluation crucial to reduce unnecessary radiation exposure to other organs. This study aimed to compare and evaluate the absorbed dose to patients undergoing ^{18}F -FDG sequential PET/CT imaging in the IKN using OLINDA/EXM and Geant4 MC simulation, focusing on identifying the most suitable method for clinical application and analysing whether the absorbed dose comply with the safety standard set by ICRP 128. The study involved retrospective analysis on 30 adult patients inclusive of 13 men and 17 women with mean age, weight and administered activity were 55.10 ± 14.05 years, 68.87 ± 20.99 kg and 327.61 ± 87.95 MBq respectively. OLINDA/EXM version 1.1 and Geant4 MC simulation (version 10.6.0) software were used to evaluate the absorbed doses to liver, kidney and urinary bladder. MIRD5 mathematical phantom were used in Geant4 MC simulations whereas in OLINDA/EXM, adults male and female models which the organ mass were normalized with Japanese reference model were applied. The mean absorbed dose to liver, kidneys and urinary bladder were 0.010 ± 0.006 mGy/MBq, 0.011 ± 0.004 mGy/MBq and 0.025 ± 0.047 mGy/MBq, respectively, for OLINDA/EXM. For Geant4 MC simulations, the mean absorbed dose to liver, kidney and urinary bladder were 0.009 ± 0.004 mGy/MBq, 0.011 ± 0.003 mGy/MBq and 0.073 ± 0.086 mGy/MBq, respectively. The corresponding differences between these two methods

were 10.53%, 0% and 97.96% respectively for liver, kidney and urinary bladder. Good agreements were observed between the absorbed doses in the liver and kidneys; however, Geant4 overestimated the absorbed dose in the urinary bladder. This discrepancy is due to differences in the methods used to calculate the absorbed dose, the inhomogeneous volume of the urinary bladder, and variations in the effective half-lives of the organs. Both OLINDA/EXM and Geant4 showed reliable absorbed dose estimation, as the results were in good agreement between the two methods. Even though OLINDA/EXM offers a more user-friendly interface, it is limited in terms of flexibility to simulate absorbed dose in various other clinical setups. Geant4 on the other hand, allow flexibility in simulating various dosimetry setup, however is limited in terms of user-friendly interface, especially in the clinical setting. In conclusion, the absorbed doses recorded in this study comply with the limits provided by ICRP-128, i.e., 0.021 mGy/MBq, 0.017 mGy/MBq, and 0.130 mGy/MBq, for liver, kidneys, and urinary bladder, respectively, indicating the safe use of ^{18}F -FDG for diagnostic purpose in IKN.

CHAPTER 1

INTRODUCTION

1.1 Background of the Study

Cancer is one of the leading causes of death worldwide (Almuhaideb et al., 2011). Its incidence has been increasing over the years, and the effort to reduce the cases has been ongoing for decades. According to World Health Organization (WHO), currently 24.6 million of people had cancer and in 2020, 16 million new cases will arise and 10 million died because of cancer every year (Teh & Woon, 2021). The Malaysia National Cancer Registry Report (MNCRR) (National Cancer Institute, 2019) reported an increase in the percentage of cancer cases detected in stages 3 and 4 from 58.7% between 2007 and 2011 to 63.7% between 2012 and 2016, despite government strategies for early screenings. Late detection is associated with poorer prognosis. Accurate diagnosis, staging and restaging are crucial for the optimal therapeutic management of cancer patients.

Various methods are used to diagnose cancer, including 2-dimension (2D) and 3-dimension (3D) imaging with techniques for example positron emission tomography (PET), magnetic resonance imaging (MRI), single photons emission computed tomography (SPECT), computed tomography (CT) and X – ray imaging besides analysing the molecular signatures of cancer cells (Frangioni, 2008). Positron emission tomography/Computed tomography (PET/CT) combines PET scanner with CT scanner to acquire images in the same session, resulting a series of superimposed images. Fluorine-18 (^{18}F) (97 % β^+ decay, 109.7 min half-life, 635 keV, β^+ energy), is a commonly used radioisotope in PET/CT. PET with 2 – deoxy – 2 [fluorine-18] fluoro – D – glucose (^{18}F -FDG), an analogue of glucose, provides valuable functional

information based on the increased glucose uptake and glycolysis of cancer cells and depicts metabolic abnormalities before morphological alterations occur (Almuhaideb et al., 2011). The use of ^{18}F -FDG in PET modalities has been proved to be effective in diagnosis, response evaluation and recurrence detection as well as medication prediction in nuclear medicine (Abdelhalim et al., 2020). Higher uptake of ^{18}F -FDG corresponds with the increase of glucose metabolism in lesion cells indicating a signal of detection of tumour viability (Abdelhalim et al., 2020).

The dosimetry approach commonly used in ^{18}F -FDG at PET/CT involves calculating the absorbed dose to organs and tissues using standardized methods based on the patient's administered activity of ^{18}F -FDG. This is typically accomplished by acquiring CT images for anatomical localization and PET for functional assessment of organs, followed by calculating the absorbed dose using software (Quinn et al., 2016). These software tools consider factors such as the patient's body composition, organ size, and ^{18}F -FDG distribution when generating calculation that will ensure the radiation exposure from ^{18}F -FDG PET/CT remains within safe levels while providing accurate diagnostic information.

In 2013, Institut Kanser Negara (IKN) was fully established, featuring specialized facilities dedicated to the treatment and care of cancer patients as well as addressing all the growing needs related to cancer issues in the country. IKN comprises of 3 largest departments which are oncology, radiotherapy and nuclear medicine. PET/CT and cyclotron modalities were available in this institute and had been providing ^{18}F -FDG PET/CT scans since 2006.

1.2 Problem Statement

The use of ^{18}F -FDG in PET/CT scans has widely expanded worldwide and various studies have been conducted to address radiation protection concerns for both staff and patients. ^{18}F -FDG is a major positron (a positively charged electron) emitter. This positron in turn interacts with a free electron and an annihilation reaction occurs, resulting in the production of two 511-keV photons, emitted at almost 180° to each other. Energy emitted from the annihilation reaction is high and were among the highest radionuclides energy emitted in most of nuclear medicine department worldwide. Currently, PET/CT with ^{18}F -FDG has become crucial in oncological imaging. However, this scanning method exposes patients to ionizing radiation, which can lead to biological effects, with cancer is always being a significant concern (Zabarmawi, 2024). As ^{18}F -FDG is primarily used for diagnostic imaging, dosimetry assessment is crucial to minimize radiation exposure to other organs. Calculating the absorbed dose in organs with high ^{18}F -FDG uptake, such as the liver, kidneys and urinary bladder (Vangu & Momodu, 2022), is crucial for assessing radiation-related risks, as exceeding threshold limits given by Internal Commission on Radiological Protection (ICRP) 128 (Clement et al., 2015) may result in deterministic effects. There are two main methods of internal dose estimation which is analytical calculation and Monte Carlo simulation (Tajik-Mansoury et al., 2016). Absorbed dose calculations in clinical are most commonly performed using analytical methods, such as established nuclear medicine software such as Organ Internal Dose Assessment/Exponential Modelling (OLINDA/EXM), while Monte Carlo (MC) simulations are less frequently utilized. MC simulation methods are considered the gold standard for dosimetry calculation including internal dose distribution, although requires some computational

skills (Neira et al., 2020) . The absorbed dose recorded is both methods should not above the limits provided by ICRP-128.

1.3 Aim & Objectives

The main aim of the study was to compare and evaluate the internal dosimetry of patients undergoing ^{18}F -FDG PET/CT imaging in IKN using OLINDA/EXM and Geometry and tracking (Geant4) monte carlo (MC) simulations. The specific objectives are as follows:

- i. To evaluate retrospectively 30 patients' demographic and tomographic data related to ^{18}F -FDG PET/CT imaging in the IKN in 2021.
- ii. To estimate the absorbed dose to source and target organs following ^{18}F -FDG administration using OLINDA/EXM software.
- iii. To estimate the absorbed dose to source and target organs following ^{18}F -FDG cases using Geant4 MC simulation.
- iv. To compare between the absorbed dose estimated using the OLINDA/EXM software and the Geant4 MC simulation.

1.4 Scope of study

This retrospective study involved the use of 2021 IKN's patients' data of ^{18}F -FDG whole body scan (WBS) with single sequential scan and only adult patient were selected in this study. Medical Image Merge (MIM) software was used as quantitative imaging tools, while OLINDA/EXM that were based on Medical Imaging Radiation Dose (MIRD) and Geant4 MC simulation were used for absorbed dose calculation and simulation, respectively. Only absorbed doses to the liver, kidneys and urinary bladder were estimated in this study.

1.5 Limitation of study

The limitation of the study includes model assumptions in simulations, computational resources constrain, radiobiological uncertainty, limited patient specific data and small number of sample size.

1.6 Thesis organization

This thesis consists of five chapters. Chapter 1 presents an introduction to the thesis. It also discusses the importance of radiation dosimetry assessment in clinical applications and the importance of having patient dose evaluation. This Chapter also presents the problem statement, objectives, limitation and scope of the study. Chapter 2 discusses the basic concept of radiation, types of radionuclides had in the medical and briefly described the society that involve giving baseline based on scientific research in radiation dosimetry. In this chapter also describe generally types of MC simulation available that were used in radiation dosimetry estimation. Chapter 3 discusses materials and methodology involved in this study. The data collection is explained in this Chapter. The dosimetry calculation for both methods were described in this chapter. Chapter 4 presents results and discussions of this study. The result of this study covers dosimetry by calculation which focused on absorbed dose of using OLINDA/EXM and Geant4. The obtained result also attached with dedicated graphs and tables to ensure well explanation in the discussion section. The statistical analysis is also discussed in this Chapter. Chapter 5 presents the conclusions and recommendations for future works.

CHAPTER 2

LITERATURE REVIEW

2.1 Cancer in Malaysia

Malaysia's population, consisting of slightly over 30 million people, is multi-ethnic, with the three largest ethnic groups being Malays (69.1%), Chinese (23.0%), and Indians (6.9%) (Schliemann et al., 2020) and had a 74.9-year life expectancy at birth (Rajadurai et al., 2020). Cancer is fourth biggest killer in Malaysia according to the Malaysia Study on Cancer Survival (MySCan) and this mainly is due to Malaysians are practicing western lifestyle that leading to cancer risk. Sugar, sweetened condensed milk, and native sweets are extensively consumed in Malaysia, and more than half of the population is overweight or obese. World Health Organization (WHO) estimates that over 40% of Malaysian males smoked in 2016 (Schliemann et al., 2020). Nearly half of all adult male smoke and statistic shows that more than 90% of male lung cancer patients have smoked at some point in their lives compared to all young female lung cancer patient who are never smoke (Rajadurai et al., 2020).

Cancer is the second biggest cause of mortality worldwide, with an estimated 9.6 million deaths due to cancer in 2018. Poor awareness and knowledge of the signs and symptoms of common malignancies is likely to abandon seeking aid, diagnosis, and treatment, resulting in poor survival results. To create health promotion initiatives aimed at reducing cancer incidence and improving early diagnosis and outcomes, its essential to assess and evaluate awareness levels and identify knowledge gaps (Schliemann et al., 2020). According to the WHO, there are currently 24.6 million people living with cancer, with 16 million new cancer diagnoses and 10 million cancer deaths expected each year by 2020 (Teh & Woon, 2021).

2.1.1 Epidemiology of Cancer in Malaysia

Cancer is a worldwide health issue and Malaysia is no exception. It is crucial to comprehend the epidemiology of cancer in Malaysia to facilitate efficient public health planning and interventions. While Malaysia has made notable progress in cancer research and management in recent years, there are persistent challenges. According to summary registry report 2012 – 2016 done by Institut Kanser Negara, IKN (National Cancer Institute, 2019), top 5 most common cancers in Malaysia within years 2007 until 2016 are breast, colorectal and lung, trachea and bronchus. There are slight increase 1.3 percent in breast cancer and 0.3 percent in colorectal from years 2012 – 2016 compare to 2007 – 2011 and a decrease in 0.4 percent for lung, trachea and bronchus cancers. The significance of cancer screening and early detection cannot be overstated in enhancing cancer prognosis. In Malaysia, a range of screening initiatives has been introduced, encompassing mammography for breast cancer and colonoscopy for colorectal cancer. Nonetheless, these programs encounter obstacles linked to accessibility and awareness, which impede their overall effectiveness.

2.1.2 Diagnosis of Cancer

The best opportunity for a cure against cancer is doing early cancer diagnosis. According to WHO, early cancer diagnosis saves lives and cuts treatment costs. Only for those at higher risk are screening for other malignancies advices. Patient advocacy groups and non-government organization (NGO) play an important role in securing and safeguarding patient's right for better cancer management (Ozmen, 2018). There are few approaches that doctor used to diagnose cancer which are from physical exam, laboratory tests, imaging tests and by biopsy. By physical exam, doctor may look for abnormalities in our body such as changes in skin colour or enlargement of an organ that could be the presence of cancer. With laboratory tests, samples such as urine and

blood needed for doctors to identify abnormalities that can be caused by cancer. Imaging tests allow doctors to examine our internal organs in a non-invasive way. Modalities such as computed tomography (CT) scan, bone scan, magnetic resonance imaging (MRI), positron emission tomography/computed tomography (PET/CT), ultrasound and X-ray are normally used in diagnosing cancer (Frangioni, 2008).

2.1.3 Treatment Options for Cancer

The type of treatment administered depends on the specific cancer type diagnosed in the patient. Treatment strategies primarily revolve around two key factors: the type of cancer and metastatic of the cancer. Some treatments are meant to cure the cancer and in some circumstances, the goal is to stop the cancer from spreading further. During cancer treatment, another treatment called palliative care is also given to reduce side effects of cancer treatments.

There are few common types of cancer treatment used such as surgery, chemotherapy, radiation therapy, hormone therapy, immunotherapy and stem cell transplant. Surgery is where doctors cut out tissue with cancer cells, chemotherapy is a special medicine that shrinks or kills cancer cells, radiation therapy is using high-energy rays to kill cancer cells. Hormone therapy is used to block cancer cells from getting the hormones they need to grow whereas immunotherapy is a treatment that works with our body's immune system to help it fight cancer cells or to control side effects from other cancer treatments. Stem cell transplant or bone marrow transplant is the treatment to replace bone marrow cells lost due to very high doses of chemotherapy or radiation therapy.

2.2 Radioactive Decay

Emission of energy in the form of ionizing radiation from the nucleus is called radioactive decay. The ionizing radiation usually are in the form of alpha particles, beta particles, gamma rays and positron. The nucleus loses energy makes it more stable transforms into a different atom which is a decay product. The atoms continue to decay into new decay products until they reach a stable state and cease to be radioactive.

2.2.1 Alpha (α) decay

Alpha (α) decay is the emission of an α particle from the nucleus. When an α particle decay occurs the radioactive nucleus changes into a different more stable nucleus, with 2 fewer protons and 2 fewer neutrons. Equation 2.1 shows the equation for alpha decay:



Where:

X is mass number

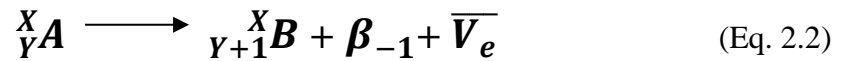
Y is atomic number

α is alpha

Alpha particles are made of large helium nuclei. They do not penetrate very far through materials, and can be stopped by just 30 cm of air a sheet of paper.

2.2.2 Beta (β) decay

Beta (β) decay is the emission of an electron from a nucleus. Emission of an electron does not change the mass number of the nuclide but does increase the number of its protons and decrease the number of its neutrons. Equation 2.2 shows the equation for alpha decay:



Where:

X is mass number

Y is atomic number

β is beta

A beta particle is a high energy electron that is emitted from the decaying nucleus. They are smaller than alpha particles so they will collide with fewer particles when travelling through a medium. This means that in beta decay, fewer particles in the medium are ionised compared to alpha decay and the beta particles are stopped over a greater distance. It takes a few cm of aluminium to stop beta particles.

2.2.3 Gamma (γ) decay

Gamma rays are photon beams with a high energy. They have no mass or charge hence they not really interact with matter. They can travel large distances through air without being stopped. A gamma ray is stopped by a few cm of lead. Because it has no electric charge, a gamma ray will travel in a straight line through magnetic and electric fields. Equation for gamma decay as shown in Eq 2.3:



Where:

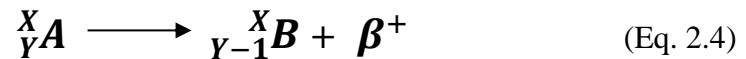
X is mass number

Y is atomic number

γ is gamma ray

2.2.4 Positron emission (β^+) decay

Positron emission (β^+) decay is the emission of a positron from the nucleus. When a β^+ decay occurs, a proton in the radioactive nucleus is converted into a neutron. Equation for positron emission as shown in Eq 2.4:



Where:

X is mass number

Y is atomic number

β^+ is positron emission

2.3 Linear energy transfer (LET)

The amount of energy that an ionising particle delivers to the substance traversed per unit distance is known as linear energy transfer (LET) in dosimetry. It discusses how radiation interacts with materials. Equation for LET as shown in equation 2.5. Higher LET causes greater biological impact and is assigned a higher Quality Factor, Q(L). Q(L) is a function of unrestricted LET specified by the International Commission on Radiation Units and Measurements (ICRU) in 1980 as:

$$L_{\infty} = \frac{dE}{dx} \quad (\text{Eq. 2.5})$$

Where:

dE is the energy

dx is distance.

The unrestricted LET, L_{∞} , is later commonly denoted by L by the ICRU in 1980 and 1993. The joule per kilogramme is the unit of absorbed dose and of all dose equivalent quantities. Later the term 'gray (Gy)' is used for this unit when reference is made to absorb dose to avoid confusion between quantities.

2.4 Radionuclide Production

Shortly after radioactivity was discovered, efforts were made to enhance its value for medical and other purposes, leading to the development of "artificial" or "man-made" radiation procedures. Radionuclides used in nuclear medicine is for diagnostic and therapeutic operations. The terms isotope and radioisotope are frequently used in nuclear medicine (Fred A. Mettler & Milton J. Guiberteau, 2019). An isotope is a set of related forms of the same element. They have the same atomic number (Z) because they have the same amounts of protons, but they have varied mass numbers (A) due to different neutron numbers.

The most widely used radionuclide in nuclear medicine is technetium-99m (^{99m}Tc), which is the same isotope as technetium-99 (^{99}Tc). The 'm' indicates that the nuclide is metastable, and therefore a nuclide is described by its isotopic form and energy state (Currie et al., 2011). Radionuclides degrade exponentially following to their half-life. Naturally occurring radionuclides have long half-lives, perhaps thousands of years to become stable long half-lives radionuclides are worthless in nuclear medicine as it will affects the total radiation received by the patients. Excessively longer half-lives will deliver the majority of the dose outside the window, and the administered dose would be too low for successful imaging or therapy as a result (Figure 2.1) radionuclides stay longer after the treatment thus, short-lived radionuclides for medical purposes are required (Currie et al., 2011)

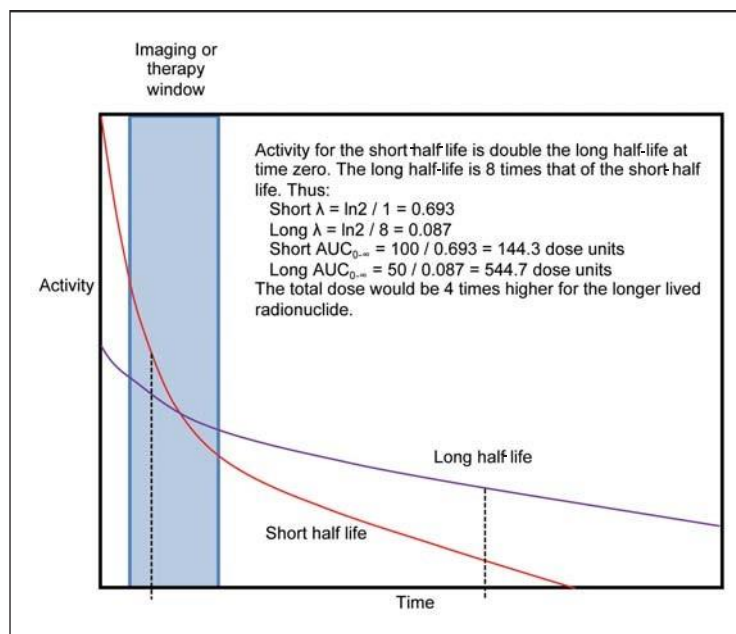


Figure 2.1 The impact of the radionuclide half-life on cumulative patient dose is illustrated in this diagram. Since radioactive decay is exponential, the area under the curve (AUC) is simply $AUC = \text{Dose} / \lambda$ where λ is $\ln 2$ divided by the half-life.

All radionuclides utilised in nuclear medicine today are created artificially in a nuclear reactor or a particle accelerator. Most hospital currently obtain their radionuclides from one of three sources: nuclear research reactors, radionuclide generators, or cyclotron facilities (Table 2.1) (Synowiecki et al., 2018).

Table 2.1 Common types of radionuclides sources.

	Nuclear Reactors	Generators	Cyclotrons
Principles of production	Fission or neutron activation transmutes target material introduced in the neutron flux field into the radionuclide of interest.	Long-lived parent radionuclide decays to short-lived daughter nuclide of interest. Elution of daughter nuclides occurs in predetermined cycles.	Irradiation of target material with charged particle beams. Inducing nuclear reactions that transform the substance into the desired radionuclide.
Transmutation base	Neutrons	Decay	p, d, t, ^3He , α or heavy ion beams

Advantages	<ul style="list-style-type: none"> -Production of neutron-rich radionuclides, mostly for therapeutic purposes. - High production efficiency. - Centralized production: a single research reactor capable of supplying enormous areas or, in certain situations, the entire world. 	<ul style="list-style-type: none"> - there is no need for logistics because everything is on site. - Mostly long shelf life - simple to use - After use, majority of radioactive waste is returned to the producer. 	<ul style="list-style-type: none"> - Production of proton rich elements used as β^+ emitters for PET scans. - Back-up chains are possible due to decentralised production. - long term availability - In most situations, high specific activity is present. - Small long lived radioactive waste.
Disadvantages	<ul style="list-style-type: none"> -high investment cost - high operating expenses -There is a significant amount of long-lived radioactive waste. - long period of inactivity - Trouble recoveries in case of unplanned downtime. - Concerns about public safety 	<ul style="list-style-type: none"> - Cycles of supplies are made according to the frequency of elution. Internal use must be scheduled accordingly. - In the eluted product, there are trace contaminants of the long-lived parent nuclide. 	<ul style="list-style-type: none"> - For short-lived generated radionuclides, a regional network of cyclotrons and significant logistics are required. - radionuclide production is limited according on the installed energy beam.

2.5 Introduction to Nuclear Medicine

The expansion of clinical applications in nuclear medicine, NM has been followed by the emergence of a multidisciplinary culture that has paid close attention to the entire range of safety concerns (Marengo et al., 2022). Radiation safety is of utmost important in nuclear medicine. Patients can find assurance in the fact that radiation exposure during diagnostic NM procedures is carefully regulated and

supervised, with a primary focus on safeguarding their well-being throughout the entire process. Insufficient communication before diagnostic imaging procedure leads to unfavourable patient experiences (Jacob et al., 2015), prompting efforts to improve patient-provider communication within medical imaging environments (Hyde et al., 2018).

Radiopharmaceuticals in NM able be delivered to patients through oral ingestion, intravenous or inhalation. These meticulously chosen radiopharmaceuticals are designed to specifically target particular tissues or organs within the body, facilitating precise diagnostic imaging and therapeutic interventions.

NM utilized two primary imaging methodologies, Single-photon emission computed tomography (SPECT) and Positron emission tomography (PET). These techniques empower medical professionals and technologists to capture imaging detailing the body's internal processes and functions at a molecular scale. SPECT relies on gamma rays emitted from radiopharmaceuticals, while PET employs positrons. These sophisticated imaging modalities offer distinctive perspectives on the structure and function of organs and tissues.

2.5.1 Type of Radiopharmaceuticals

Radiopharmaceuticals in NM are categorized according to their intended roles and functions in medical procedures. These compounds, comprising radioactive isotopes, find application in both diagnostic imaging and therapeutic treatments. Diagnostic imaging radiopharmaceuticals refer to imaging and visualization. These substances aid medical practitioners in acquiring data pertaining to the structure and function of particular organs, or physiological processes within the body. Examples of most common diagnostic imaging radiopharmaceuticals are ^{99m}Tc , ^{111}In , ^{68}Ga and 18-Fluorine-Fluorodeoxyglucose (^{18}F -FDG). Therapeutics radiopharmaceuticals

are intricately engineered to administer therapeutic radiation precisely to targeted tissues or cells, primarily for the purpose of treating diseases such as cancer. In contrast to diagnostic imaging radiopharmaceuticals, which emit low-energy radiation suitable for imaging, therapeutic radiopharmaceuticals emit higher-energy radiation with the potential to harm or eradicate cancerous cells. Example of therapeutic radiopharmaceuticals are ^{131}I odine, ^{177}Lu tesium, ^{153}Sm arium and ^{223}Ra dium (Sgouros, 2019).

NM has seen significant improvements, ranging from new imaging modalities to the creation and manufacture of new isotopes. As the field has grown, a new classification known as theragnostic has appeared, in which diagnostic isotopes are utilised to inform and personalize a patient's treatment with a therapeutic material. Theragnostic began almost 80 years ago with the use of ^{131}I odine, a gamma and beta emitting radionuclide that has applications in both diagnosis and treatment of thyroid cancer and is still in routine clinical use today, though alternatives such as ^{123}I odine, a pure gamma-emitter, or ^{124}I odine, a positron emitter, may be preferable as diagnostic agents due to their better imaging characteristics (König et al., 2021). ^{131}I odine is a radioisotope with a short radioactive half-life ($T_{1/2} = 8.03\text{d}$) that is selectively taken up by the thyroid gland and is widely used in medical diagnostics and therapeutic processes (Miszczyk et al., 2019)

Fluorine 18 stands out as the most commonly utilized radioisotope in PET radiopharmaceuticals for both clinical applications and preclinical investigations (Jacobson et al., 2015). Its notable physical and nuclear properties, including a 97% β^+ decay, a half-life of 109.7 minutes, and a positron energy of 635 keV, combined with its high specific activity and the ease of large-scale production, render it a highly

attractive nuclide for radiochemical labelling and molecular imaging purposes (Jacobson et al., 2015).

2.5.2 Nuclear Medicine Modalities

At the heart of NM, SPECT is a remarkable imaging modality. SPECT scan imaging utilizes radionuclides emitting γ photons or bremsstrahlung photons, which can be captured using γ camera (Dyer et al., 2024). SPECT images offer a three-dimensional view of the distribution of radiopharmaceuticals, providing insights into organ function and abnormalities. SPECT is invaluable in myocardial perfusion imaging to assess cardiac health, bone scans for detecting fractures or tumours, and brain imaging for neurological conditions. SPECT has lower spatial resolution compared to PET but it still provides crucial cross-sectional imaging of radionuclide distribution at a more affordable price per scan (Dyer et al., 2024). PET imaging utilizes radiopharmaceuticals that emit positrons, illuminating regions of heightened metabolic activity within the body and unveil molecular-level details. This technique assumes a critical role in the detection and staging of cancer, neurological research and cardiac assessments, providing unparalleled insights into disease mechanisms.

The services in NM such as in stress and multimodality imaging has increases especially for Positron emission tomography/Computed tomography (PET/CT) and Positron emission tomography/Magnetic resonance imaging (PET/MRI) (Khouqeer, 2022). These combined modalities offer a comprehensive perspective by merging functional insights from NM with anatomical intricacies from CT scans. This synergistic approach assists in precisely identifying abnormalities, enhancing diagnostic precision, and streamlining treatment planning, particularly in the field of oncology and cardiology. PET has been performed using a variety of radionuclides in spite of its growing popularity (Karimipourfard et al., 2022).

Accurate quantitative image analysis has been established using current hybrid imaging equipment of PET/CT, PET/MRI and Single-photon emission computed tomography/computed tomography (SPECT/CT). These were supported by reliable calibration, improved dual imaging acquisition and modern reconstruction techniques. This provides for a more precise estimate of tumour burden and normal tissue dosimetry for each treatment cycle, allowing for better customization, avoiding over- or under-dosing, and improving therapeutic effectiveness (König et al., 2021). As technology progresses and research thrives, it is unquestionable that NM modalities will assume an increasingly central role in shaping the future of healthcare.

2.6 Medical Internal Radiation Dosimetry (MIRD)

NM is specialized discipline committed to delving into the intricate mechanisms of the human body, diagnosing ailments and customizing treatments with remarkable precision. At the heart of NM lies the indispensable tool known as MIRD. MIRD is a technique employed to calculate the absorbed dose within a target organ resulting from one or multiple source organs (Vasquez-Arteaga et al., 2023). MIRD represents a quantitative discipline, a methodical approach that measures the absorption, distribution and elimination of radiation in the human body following the administered of radiopharmaceuticals. It encompasses mathematical models, computational algorithms and imaging data to gauge radiation dose that affecting different organs and tissues. Dosimetry involves the precise evaluation of radiation doses that patients receive from the administration of radiopharmaceuticals (Boice Jr et al., 2011).

Dosimetry calculations are primarily based on Monte Carlo (MC) simulations using pre-programmed phantoms. In contrast, measurement-based dosimetry, also referred to as external exposure, involves assessing dose from an external radiation

source. The conceptual foundations of dosimetry—including quantities, units, equations, methods, and techniques—have been established by reputable organizations such as the International Commission on Radiological Protection (ICRP), MIRDO, and the Radiation Dose Assessment Resource (RADAR). These efforts collectively contribute to the standardization of dosimetry results.

Internal radionuclide absorbed dose calculations are employed to evaluate the stochastic risks associated with diagnostic nuclear medicine and the deterministic risks to normal tissues in therapeutic nuclear medicine. For diagnostic applications, these dose calculations follow the methodology established by the MIRDO committee (Grimes & Celler, 2014)

2.6.1 Absorbed Dose, D

Absorbed dose is defined as a measurement on the amount of radiation energy absorbed in a target tissue per unit mass. The System International (S.I) unit is in Gray (Gy) as shown in Eq 2.6:

$$D = \frac{dE}{dm} = 1 \text{ Gy (J kg}^{-1} \text{)} \quad (\text{Eq. 2.6})$$

Where:

dE is energy (J)

dm is organ mass (kg)

In internal dosimetry calculation system, we assume the tissue has uniform distribution of radioactive material using a generic Eq 2.7:

$$D = \frac{k \tilde{A} \sum_i n_i E_i \phi_i}{m} \quad (\text{Eq. 2.7})$$

Where,

D is absorbed dose (Gy)

\tilde{A} is cumulated activity (MBq-sec)

n_i is number of radiations with energy, E emitted per nuclear transition

E_i is energy per radiation (MeV)

ϕ_i is fraction of energy absorbed in the target

m is mass of target region (g or kg)

k is proportionality constant (Gy-kg/MBq-sec-MeV)

With S value formula:

$$S = \frac{k \sum_i n_i E_i \phi_i}{m} \quad (\text{Eq. 2.8})$$

MIRD has simplified the Equation 2.7 and 2.8 in equation 2.9:

$$D = \tilde{A} \cdot S \quad (\text{Eq. 2.9})$$

where:

\tilde{A} is the cumulated activity in source organ

S is a value derived from an appropriate phantom and Monte Carlo simulation

The absorbed fraction (ϕ) represents the fraction of radiation energy absorbed by a target organ per unit of radiation energy emitted by the source organ. Its value ranges between 0.0 and 1.0 ($0.0 \leq \phi \leq 1.0$). Source organs typically have concentrations higher than the average body concentration, depending on the geometry of the source and target. (Monte Carlo method). The theoretical calculation of absorbed dose involves the use of absorbed fraction, specific absorbed fraction, source and target tissues, and compartmental models that describe the biokinetic distribution of the injected activity.

(Bolch et al., 2009). MIRD organisational use above Equation (2.8 and 2.9) in their calculation. While RADAR has modified the equation to be simpler in Equation 2.10:

$$D = N \times DF \quad (\text{Eq. 2.10})$$

where,

N is number of disintegrations in the source

DF is dose factor

$$DF = \frac{k \sum_i n_i E_i \phi_i W_R}{m} \quad (\text{Eq. 2.11})$$

where,

W_R is radiation weighting factor

The Dose Factor (DF) is formulated using the function of the radiation-weighting factor (WR), as defined by the International Commission on Radiological Protection (ICRP). Both the S-value and the Dose Factor (DF) are fundamentally similar in their expressions (Stabin et al., 2005)

2.6.2 Activity

Activity represents the number of decays (disintegration), N per second, and is changing over time as shown in Eq 2.13. The illustration as Figure 2.2. The S.I unit is in Becquerel (Bq) and 1 mCi = 37 MBq.

$$A_0 = \frac{\Delta N}{\Delta t} \quad (\text{Eq. 2.12})$$

Where:

ΔN is number of disintegration

Δt is time (s)

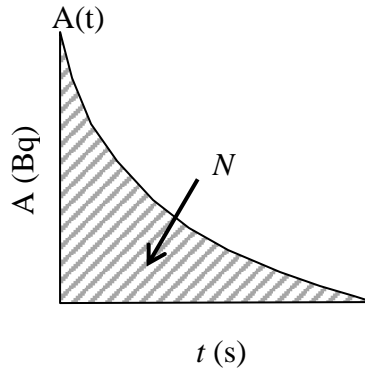


Figure 2.2 Time activity graph.

$$A(t) = A_0 \cdot \exp[-\ln(2) (t/t_{1/2})] \quad (\text{Eq. 2.13})$$

Where,

N is number of disintegrations

A_0 is initial activity taken into body (in mCi or MBq)

$t_{1/2}$ is physical half- life

t is time

A is activity

2.6.3 Cumulative Activity

Cumulative activity, \tilde{A} is a measurement of the total number of radioactivity disintegrations (N) by the decaying mode process in the source organ over the period of time or area under the time activity curve $A(t)$ as shown in equation 2.14. This expressed in SI unit as $\text{Bq}\cdot\text{sec}^{-1}$.

$$\tilde{A} = N = \int_0^{\infty} A(t) dt \quad (\text{Eq. 2.14})$$

Basic MIRD method in internal dosimetry:

$$N = \tilde{A}_T = A_0 \cdot f_h \cdot 1.44 \cdot T_e \quad (\text{Eq. 2.15})$$

Where:

A_0 is initial activity taken into body (mCi)

T_e is effective half-life (hr)

f_h is uptake fraction of A_0 deposited into organ of concern

2.6.4 Residence Time and Effective Half-Life

The definition of residence time in MIRD perspective is cumulated activity per administered activity ($\tau = \tilde{A}/A_0$) or area under the uptake curve $U(t) = A(t)/A_0$ while in RADAR perspective, the residence time is the number of total disintegrations occurring in a tissue per unit administered activity (\bar{N}) or integral of a time-activity curve for a source region. Figure 2.4 shows the illustration of the MIRD and RADAR perspective. The integral of this function has units of activity x time (e.g., Bqs^{-1} [1 Bq is 1 disintegration per second]).

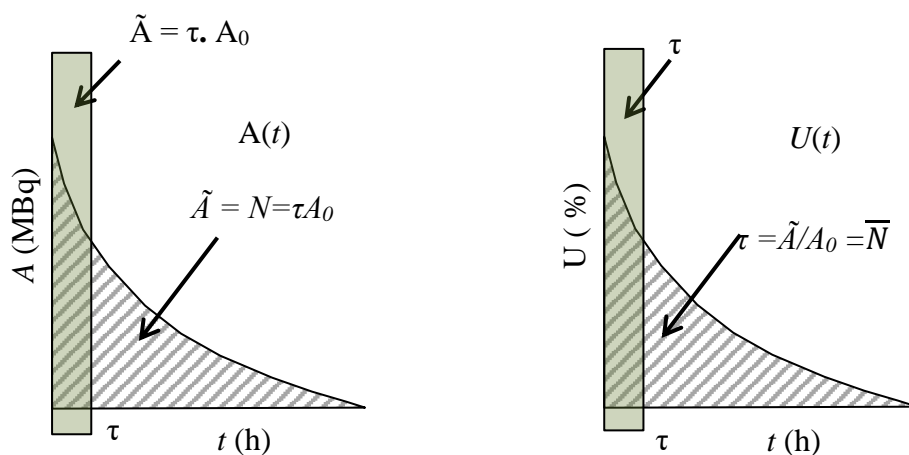


Figure 2.3 Graph of area under the curve is equal to area of rectangle.

Residence time has strong correlation with the effective half-life. Cumulated activity (Equation 2.16) and residence time (Equation 2.17) for an instant uptake and a mono-exponential decrease with an effective half-life of T_e .

$$\tilde{A} = 1.44 \cdot T_e \cdot A_{tissue} \quad (\text{Eq. 2.16})$$

$$\tau = 1.44 \cdot T_e \cdot U_{tissue} \quad (\text{Eq. 2.17})$$

where,

\tilde{A} is cumulated activity

T_e is effective half-life

A_{tissue} is administered activity

U_{tissue} is uptake activity

τ is residence time

The activity removed by radioactive decay and biological disappearance is according to Equation 2.18, which also known as effective disappearance.

$$T_e = \frac{T_b \times T_p}{T_b + T_p} \quad (\text{Eq. 2.18})$$

where,

T_p is physical half-life

T_b is biological half-life

Internal dosimetry, or dose assessment of the internal organ, is a measurement focused on the organ that will receive the exposure dosage internally. Because it is